Linear Channel Modeling and Error Analysis for Intra/Inter-Cellular Ca^{2+} Molecular Communication

A. Ozan Bicen, *Student Member, IEEE*, Ian F. Akyildiz, *Fellow, IEEE*,
Sasitharan Balasubramaniam, *Senior Member, IEEE*, and
Yevgeni Koucheryavy, *Senior Member, IEEE*

Abstract—The use of intra/inter-cellular calcium ion (Ca^{2+}) signaling for molecular communication (MC) is investigated in this paper. In particular, the elevation of the intracellular Ca^{2+} concentration upon the external excitation, i.e., Ca^{2+} wave generation, and the intercellular propagation of Ca^{2+} wave over consecutive cells are studied for information transmission. The main objective of this paper is to develop a linear channel model for intra/inter-cellular Ca^{2+} MC. In this context, the end-to-end Ca^{2+} MC system is studied under three blocks: the wave generation, the gap junctional (intercellular) propagation, and the intracellular propagation. The wave generation block captures the intracellular Ca^{2+} signaling pathway including the release of Ca^{2+} from the organelles and the buffers inside a cell, and the intake from the extracellular space. The gap junctional (intercellular) propagation block captures the Ca^{2+} transition through the gap junctions between the touching cells. The intracellular propagation block defines the effect of the cytoplasmic diffusion. Using the developed blocks for the different biophysical phenomena, the end-to-end channel gain and delay formulas are derived. Furthermore, the bit error probability is studied to reveal the impact of the detection threshold. This work provides the basis for the modeling, analysis and the design of Ca^{2+} MC systems.

Index Terms—Bit error probability, channel modeling, intercellular Ca^{2+} waves, intracellular Ca^{2+} signaling, molecular communication.

I. INTRODUCTION

MOLECULAR communication (MC) is expected to enable a wide range of applications *in vivo* including the monitoring of biochemicals, the detection of pathogens, the point-of-care diagnosis of cell anomalies, and the smart drug delivery [1]. In the literature, several different biochemical signaling mechanisms have been investigated for the information transmission using molecules, such as bacterial signal transduction [2], [3], molecular motors [4], [5], ion channels between cardiomyocytes [6], pheromones [7], drug delivery systems [8], [9], and receptor-ligand kinetics [10] in the last decade. Apart from the aforementioned molecular signaling techniques, Ca^{2+} signaling is proposed for the development of a MC system in [11]. The propagation of the Ca^{2+} signals through the consecutive cells touching each other provides an information transmission mechanism for MC as shown in Fig. 1. In this work we focus on the intra/inter-cellular Ca^{2+} signaling as the information transmission technique similar to [11].

The Ca^{2+} signals have been found to participate in many biological functions in both animal and plant cells [12]–[18]. In addition to the important role in electrically excitable muscle cells and neurons for contraction [19] and synaptic transmission [20], respectively, the regulatory role of the Ca^{2+} signals have also been observed for non-excitable cells, e.g., during fertilization in oocytes [21] and depending on hormone stimulation in hepatocytes [22], [23].

As shown in Fig. 1, for MC with Ca^{2+} signals, the transmitter side is composed of the external excitation and the wave generating cell(s). The external excitation such as extracellular elevation of the agonist or Ca^{2+} concentration leads to increase in the internal Ca^{2+} concentration, i.e., the generation of the Ca^{2+} wave, at the source cell. In Ca^{2+} signaling, the touching neighbor cells can serve as a communication channel, and connect the transmitter side and the receiver side. The Ca^{2+} wave is transferred to the touching neighbor cells through the gap junctions, which results in the intercellular Ca^{2+} wave propagation. Through the consecutive cells, the Ca^{2+} wave propagates until it reaches the receiver side which can be composed of a measurement system, e.g., based on the light emission and confocal microscopy [24]. The receiver samples the received Ca^{2+} level and performs the desired actuation, such as for example, drug injection [25].

For the end-to-end Ca^{2+} MC system, the following scenario can be considered as an example: a sensor placed beneath
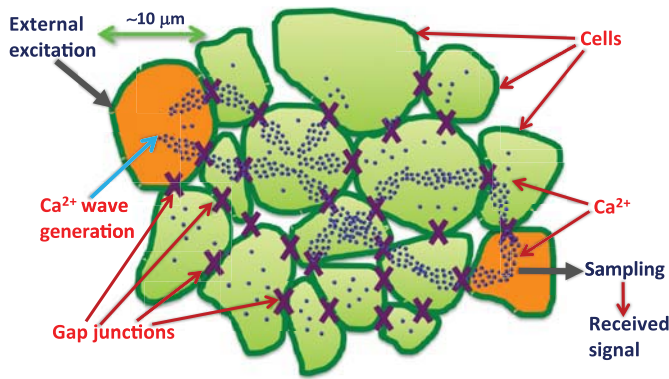
Fig. 1. Conceptual illustration of the Ca^{2+} signaling over consecutive cells touching each other. First, the Ca^{2+} level is elevated, i.e., Ca^{2+} wave is generated in the cell where the external excitation is applied. Then, the Ca^{2+} wave repetitively propagates through the gap junctions and diffuses inside the cytoplasm. The Ca^{2+} wave reaches to the destination cell where the samples are taken and the received signal is deduced.

the smart tissue can trigger elevation of Ca^{2+} level. Then, this wave can propagate through the tissue towards the cells next to skin. The samples from cells immediately below the skin can be utilized to detect any transmitted information from the deep tissue. The use of intercellular Ca^{2+} waves for the information transmission can bring significant advantages for the applications of MC in the health monitoring and point-of-care diagnosis systems. However, the Ca^{2+} wave is exposed to the channel impairment effects while propagating through the multi-cellular biophysical environment as shown in Fig. 2, which represents the unique features for MC. Therefore, a thorough analysis of the multi-cellular biophysical dynamics is required to realize the MC with the intercellular Ca^{2+} waves.

The mathematical modeling of Ca^{2+} signaling mechanisms has been a research field of interest in recent years. Many intracell and intercell models with different biophysical details have been proposed in accordance with the experimental evidence [26]–[28]. In addition to the biophysical modeling, various approaches have been developed recently under MC domain for the simulation of different factors contributing to the Ca^{2+} signaling mechanisms to evaluate the MC performance [11], [29], [30]. Based on the activity of enzymes in the intracellular Ca^{2+} signaling pathway, the intercellular Ca^{2+} waves can propagate in a diffusive manner through the gap junctions and the regenerative factors can be neglected at the intermediate cells along the propagation path [36]. Using this fact, aside from the studies based on the simulation, the objective of this study is to develop a linear channel model that captures the attenuation and delay characteristics of MC with intercellular Ca^{2+} waves. A linear channel model can be solved directly, and the methodologies developed to assess performance of linear communication systems can also be applicable for MC with intercellular Ca^{2+} waves, e.g., detection and estimation theory and information theory for linear channels [31], [32]. To the best of our knowledge, this is the first attempt to develop a linear channel model for the Ca^{2+} MC that considers the end-to-end effects of intracellular wave generation and its relation to the intercellular signaling.

In this paper, first, the biophysical mechanisms of Ca^{2+} signaling are elaborated for the electrically non-excitable

cells. Then, the linear modeling of the end-to-end MC with intra/inter-cellular Ca^{2+} signaling is studied under the three blocks: Ca^{2+} wave generation, the intercellular gap junctional propagation, and the intracellular diffusion propagation as shown in Fig. 2. The wave generation block is developed based on the intracellular Ca^{2+} signaling pathway including the release of Ca^{2+} from the organelles (stores) and the buffers inside a cell, and the intake from the extracellular space. The gap junctional propagation block incorporates the Ca^{2+} ion transition through the gap junctions among the touching cells addressing the successful gap junction opening probability, the gap junctional permeability, and the gap junctional delay. The intracellular propagation block includes the effect of the cytoplasmic diffusion. The receiver samples the peak value of the Ca^{2+} concentration at the cell N as shown in Fig. 2. Furthermore, the noise effects due to the biochemical reactions in Ca^{2+} wave generation and the imperfect measurements at the receiver are also incorporated. Consequently, a linear end-to-end channel model is obtained for the Ca^{2+} molecular communication systems.

Additionally, using the developed linear channel model, the bit error probability is studied for the pulse amplitude modulation (PAM). The impact of the pulse level difference on the end-to-end binary information transmission performance is specifically investigated. Numerical results are presented to provide an insight into the impact of the biophysical parameters on the channel characteristics and the error probability for MC with intra/inter-cellular Ca^{2+} signaling. In particular the Ca^{2+} wave propagation range is studied in terms of the number of cells along the propagation path.

The linear channel modeling and the bit error probability analysis are aimed to facilitate the modeling, analysis and the design of information transmission schemes considering the biophysical dynamics of the Ca^{2+} MC systems. Furthermore, the linear channel modeling effort can enable the reverse engineering of the biological systems with intra/inter-cellular Ca^{2+} signaling and estimation of the biophysical parameters of the tissues.

The paper is organized as follows. Section II gives the foundations on the biophysical mechanisms of the Ca^{2+} signaling. The linear channel modeling framework for intra/inter-cellular Ca^{2+} MC is developed in Section III. Section IV presents the analysis for the bit error probability. The numerical results are given in Section V. Lastly, the paper is concluded in Section VI.

II. BIOPHYSICAL FOUNDATIONS OF Ca^{2+} SIGNALING

The Ca^{2+} signaling systems can regulate a wide range of cellular processes and work at different time-scales [26]. For example, Ca^{2+} signaling operates in the milliseconds range at the synaptic junction, while protein synthesis and cell division require Ca^{2+} signaling mechanisms to operate in the range varying from minutes to hours. In the following, we provide an overview of the intracell and the intercellular Ca^{2+} dynamics.

A. Intracellular Ca^{2+} Signaling Pathway

Here, we focus on Ca^{2+} transients in the electrically non-excitable cells. The level of Ca^{2+} in the cytoplasm is
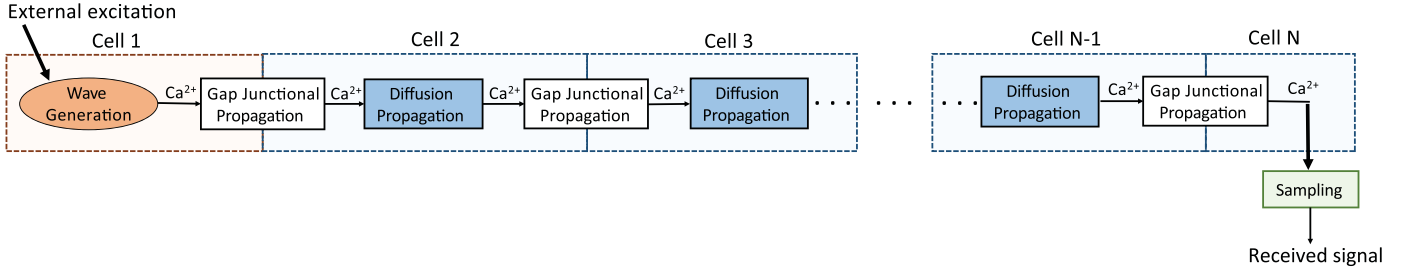
Fig. 2. Block diagram representation of the intra/inter-cellular Ca^{2+} molecular communication channel. The blocks represent the different biophysical phenomena, i.e., the wave generation, the gap junctional (intercellular) propagation, and the diffusion (intracellular) propagation, that the information carrying Ca^{2+} wave undergoes during the end-to-end propagation.

TABLE I
DEFINITION AND VALUES OF THE BIOPHYSICAL PARAMETERS

Parameter	Value
D_{Ca} (Ca^{2+} diffusion constant for cytoplasm)	$20 \times 10^{-6} \mathrm{m}^2/\mathrm{sec}$
P_{Ca} (Gap junction permeability for Ca^{2+})	$5 \times 10^{-6} \mathrm{m}/\mathrm{sec}$
K_7 (Dissociation constant of the plasma membrane calcium pump)	$0.6 \mu M$
k_5 (Rate of calcium influx from the external medium)	$0.000158 \mathrm{sec}^{-1}$
V_6 (Maximum rate of the plasma membrane calcium pump)	$1.5 \mu M/\mathrm{sec}$
h (Fractional activity of the channels in the store and plasma membrane ($h_0 \leq h \leq 1$))	1
h_0 (Basal fractional activity of the channels in the store and plasma membrane)	0.4
C_{ext} (Extracellular calcium concentration)	$1500 \mu M$
C_{cyt}^{init} (Initial cytoplasmic Ca^{2+} concentration)	$0.5 \mu M$

determined by the on and off reactions that cause increase and decrease in Ca^{2+} concentration, respectively. The Ca^{2+} signaling pathway is composed of different reactions based on the type of the cell.

Various types of stimuli including extracellular agonists and intracellular messengers can cause elevation of the Ca^{2+} level in the cytoplasm. The Ca^{2+} is provided by the internal stores or the external medium. As a result of the on and off reactions in the signaling pathway, the Ca^{2+} pulse is generated. In the literature, a set of mass balance equations are used to model each Ca^{2+} variable in the intracellular Ca^{2+} signaling pathway [26], [27].

In this work, a model with three types of Ca^{2+} concentration variables, i.e., the cytoplasmic C_{cyt}, the store (organelles) calcium C_{str}, and calcium buffers B, is utilized from [33]. The extracellular Ca^{2+} that enters the cell from the outside is taken as the external excitation source for the Ca^{2+} signaling pathway. The kinetic model is described by the following equations [33]:

$$\frac{\partial C_{str}}{\partial t} = -k_1(h + h_0)(C_{str} - C_{cyt}) + V_3 \frac{C_{cyt}^2}{K_4^2 + C_{cyt}^2} \quad (1)$$

$$\frac{\partial C_{cyt}}{\partial t} = k_1(h + h_0)(C_{str} - C_{cyt}) - V_3 \frac{C_{cyt}^2}{K_4^2 + C_{cyt}^2}$$
$$+ k_5(h + h_0)(C_{ext} - C_{cyt}) - V_6 \frac{C_{cyt}^2}{K_7^2 + C_{cyt}^2}$$
$$- k_2 C_{cyt} B + k_2 (B_{total} - B) \quad (2)$$

$$\frac{\partial B}{\partial t} = -k_2 C_{cyt} B + k(B_{total} - B) \quad (3)$$

where k_1 is the rate of Ca^{2+} release and influx for the store, k_2 is the binding constant of Ca^{2+} for the buffers, V_3 is the

maximum rate of Ca^{2+} intake to the store, K_4 is disassociation constant for the store calcium, B_{total} is the total calcium buffer concentration, and the definitions as well as the values of the other biophysical parameters are listed in Table I. The values of the biophysical parameters listed in Table I are based on the values in [33]. The change of Ca^{2+} in store organelles with respect to the store release and take in rate constants, and C_{cyt} is described in (1). The balance equation in (2) relates the change of cytoplasmic Ca^{2+} to the Ca^{2+} concentration in the intracellular store, the free buffer in the cytoplasm, and extracellular matrix, as well as their corresponding release and take in rate constants. The process of Ca^{2+} binding to the free buffer in the cytoplasm is defined in (3).

B. Intercellular Ca^{2+} Signaling Through Gap Junctions

The intercellular Ca^{2+} signaling can either provide the synchronization of the Ca^{2+} level with the neighboring cells or serve as long-range signaling pathway via wave propagation. The synchronization of Ca^{2+} level in cells has been studied via both analytical and experimental studies [34]. For example, in response to hormones, i.e., vasopressin and noradrenalin. The Ca^{2+} level in hepatocytes is shown to be synchronized via gap junctional coupling [34]. Apart from synchronization, the Ca^{2+} wave propagation can provide information transfer via forming a signaling pathway over touching neighboring cells. During the course of this work, we focus on the Ca^{2+} wave propagation over consecutive cells.

The Ca^{2+} wave propagation speed of the gap junctional path is much faster than the propagation by diffusion across the extracellular space [19], [35]. Therefore, the extracellular propagation is neglected, and the gap junctional signal propagation has been the interesting feature to capture Ca^{2+} wave propagation characteristics in analytical modeling efforts [36].

Additionally, the intercellular Ca²⁺ wave propagation is controlled by the internal Ca²⁺ wave regeneration mechanisms in the intermediate cells along the propagation path. The intermediate cells can enhance the intercellular Ca²⁺ wave via the internal Ca²⁺-induced Ca²⁺ release process. The Ca²⁺ wave regeneration at the intermediate cells is attributed to the gap junctional propagation of the elevated IP₃ together with Ca²⁺ wave from the stimulated cell and the activity of the PLCδ enzyme at the intermediate cells [36]. PLCδ activity determines the IP₃ production in the presence of Ca²⁺. In this paper we assume the PLCδ enzyme activity is low, such that the Ca²⁺ wave regeneration at the intermediate cells is negligible. We focus on solely Ca²⁺ propagation through the gap junction connections between the touching cells.

III. LINEAR END-TO-END CHANNEL MODEL

We model the Ca²⁺ signaling based on the elementary parts that form the end-to-end propagation path as shown in Fig. 2. The information is assumed to be encoded in the amplitude of the Ca²⁺ wave by signal transduction [37]–[39], and the extracellular Ca²⁺ (C_{ext}) is assumed as external excitation factor. We first model the wave generation according to the intracellular signaling pathway given in Section II-A. Then, we model the intercellular Ca²⁺ wave propagation via gap junctional transfer of Ca²⁺ through touching neighboring cells. We also study the intracellular propagation of Ca²⁺ waves via diffusion. Lastly, the noise effects on intercellular Ca²⁺ waves are discussed, and the end-to-end channel model is presented.

A. Ca²⁺ Wave Generation

Here, based on the quantitatively described intracellular signaling pathway in Section II-A, we study the Ca²⁺ wave generation dynamics. The cytoplasmic Ca²⁺ level is elevated at the source cell where the external stimuli is applied. Here, we investigate the steady-state and the transient response of the Ca²⁺ wave generation to develop a linear model and obtain the delay for the wave generation elementary block.

The steady-state response is defined as

$$\eta = \lim_{t \to \infty} C_{\text{cyt}}(t) \tag{4}$$

where C_{cyt} is the cytoplasmic Ca²⁺ concentration. To obtain the steady-state response, we set the time derivatives to 0 in (1), (2), and (3) and obtain the following set of equations:

$$0 = V_3 \frac{C_{\text{cyt}}^2}{K_4^2 + C_{\text{cyt}}^2} - k_1(h + h_0)(C_{\text{str}} - C_{\text{cyt}}) \tag{5}$$

$$0 = k_1(h + h_0)(C_{\text{str}} - C_{\text{cyt}}) - V_3 \frac{C_{\text{cyt}}^2}{K_4^2 + C_{\text{cyt}}^2} - k_2 C_{\text{cyt}} B$$
$$+ k_{-2}(B_{\text{total}} - B) + k_5(h + h_0)(C_{\text{ext}} - C_{\text{cyt}})$$
$$- V_6 \frac{C_{\text{cyt}}^2}{K_7^2 + C_{\text{cyt}}^2} \tag{6}$$

$$0 = k_{-2}(B_{\text{total}} - B) - k_2 C_{\text{cyt}} B \tag{7}$$

where the definitions of the parameters are listed in Table I. Under the biophysical condition steady-state response is much
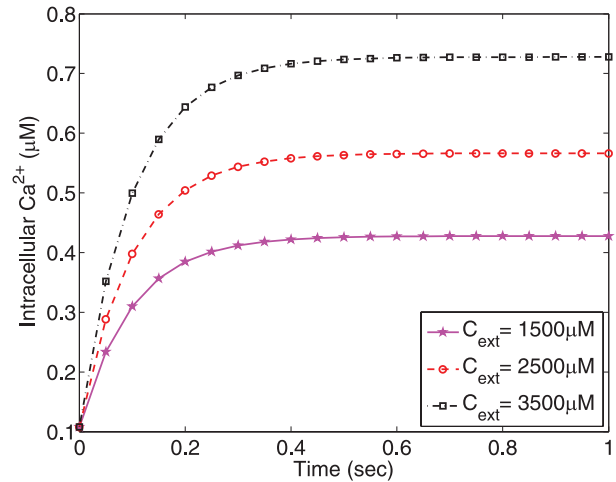

Fig. 3. The intracellular Ca²⁺ wave generation with respect to the different extracellular Ca²⁺ excitation levels.

less than the external Ca²⁺ concentration ($\eta \ll C_{\text{ext}}$), the steady-state value, i.e., η, can be obtained as [33]

$$\eta = K_7 \sqrt{\frac{k_5(h + h_0)C_{\text{ext}}}{V_6 - k_5(h + h_0)C_{\text{ext}}}}. \tag{8}$$

The transient response of the Ca²⁺ wave generation is approximated via using the solution of a first order linear differential equation as

$$C_{\text{cyt}}(t) \approx C_{\text{cyt}}^{\text{init}} + (\eta - C_{\text{cyt}}^{\text{init}})(1 - e^{-t\beta}) \tag{9}$$

where $C_{\text{cyt}}^{\text{init}}$ is the initial cytoplasmic Ca²⁺ concentration, β is the elevation rate of cytoplasmic Ca²⁺. The transient Ca²⁺ elevation is illustrated based on (9) in Fig. 3 for $\beta = 10\text{s}^{-1}$, $C_{\text{cyt}}^{\text{init}} = 0.5$ μM, and extracellular calcium values, i.e., C_{ext}, of 1500 μM, 2500 μM, and 3500 μM. For the numerical results, the parameter values are given in Table I.

Since the steady-state is reached at $t = \infty$, to calculate the delay at the generation block, we use the 90% of the steady-state value, i.e., 0.9η, which is given as

$$C_{\text{cyt}}^{\text{peak}}(t) = 0.9\eta. \tag{10}$$

Using (9), we obtain

$$0.9\eta = C_{\text{cyt}}^{\text{init}} + (\eta - C_{\text{cyt}}^{\text{init}})(1 - e^{-\tau_{\text{gen}}\beta}). \tag{11}$$

Finally, the wave generation delay τ_{gen} is obtained from (11) as

$$\tau_{\text{gen}} = -\frac{1}{\beta} \log\left(1 - \frac{0.9\eta - C_{\text{cyt}}^{\text{init}}}{\eta - C_{\text{cyt}}^{\text{init}}}\right). \tag{12}$$

For different intracell Ca²⁺ signaling pathways, the steady-state and transient response can be obtained following the provided approach in this section. Similarly, the provided approach to calculate the wave generation delay can be used for different intracellular Ca²⁺ signaling pathways by exploiting the steady-state response assumption. Therefore, the additional wave generation blocks can be developed by using the provided approach here based on the selected empirical model of the intracellular Ca²⁺ signaling.

B. Intercellular Gap Junctional Propagation

Here, we study the gap junctional propagation of Ca^{2+} signals. The intercellular gap junctional propagation gain is calculated for the N cells along the shortest delay path between the source where the cell Ca^{2+} waves are generated and the last cell where the samples are taken. The gap junctions exist at the borders of touching neighboring cells. Here, we extend the model of gap junctional Ca^{2+} wave propagation in [36] considering the time-scale of Ca^{2+} transition.

The spatial change of the Ca^{2+} concentration through the gap junctions between the $n-1$th and nth cell can be described via the following

$$-D_{Ca}^{(n)}\frac{\partial C_{cyt}^{(n)}}{\partial x}|_{x=l_{jct}^{(n)}} = \frac{P_{Ca}^{(n)}}{\tau_{gap}^{(n)}}\Big(C_{cyt}^{(n-1)}(l_{jct}^{-,n-1}, \tau_{jct}^{-,n-1}) \\ - C_{cyt}^{(n)}(l_{jct}^{+,n}, \tau_{jct}^{-,n})\Big) \quad (13)$$

where n is the cell number along the propagation path, $D_{Ca}^{(n)}$ is the diffusion constant for Ca^{2+}, $P_{Ca}^{(n)}$ is the permeability of the gap junction, $l_{jct}^{(n)}$ is the gap junction position, $\tau_{jct}^{(n)}$ is the time instant Ca^{2+} wave reaches to the gap junctions between the $n-1$th and the nth cell along the propagation path, $C_{cyt}(l_{jct}^{-,n-1}, \tau_{jct}^{-,n-1})$ represents the Ca^{2+} level in the cell where Ca^{2+} diffuses from, and $C_{cyt}(l_{jct}^{+,n}, \tau_{jct}^{-,n})$ represents the Ca^{2+} level in the cell where Ca^{2+} diffuses towards.

We assume that the initial Ca^{2+} concentration in the touching neighboring cells before the intercellular wave propagation is on a negligible level. Hence, we set

$$C_{cyt}^{(n)}(l_{jct}^{+,n}, \tau_{jct}^{-,n}) = 0. \quad (14)$$

Accordingly, we obtain the transition rate of Ca^{2+} to the next cell as

$$-\frac{\partial C_{cyt}^{(n)}}{\partial x}|_{x=l_{jct}^{(n)}} = \frac{1}{\tau_{gap}^{(n)}}\frac{P_{Ca}^{(n)}}{D_{Ca}^{(n)}}C_{cyt}^{(n-1)}(l_{jct}^{-,n-1}, \tau_{jct}^{-,n-1}). \quad (15)$$

The gap junctions are activated via the elevation of the Ca^{2+} concentration level inside the cell. Ca^{2+} ions are transferred to the next cell during this open interval of gap junctions, which is represented by $\tau_{gap}^{(n)}$ and in the range of a few hundred milliseconds. We denote the effective gap junctional transition rate of Ca^{2+} wave by θ_n, and is defined based on (15) as

$$\theta_n = \frac{1}{\tau_{gap}}\frac{P_{Ca}^{(n)}}{D_{Ca}^{(n)}}. \quad (16)$$

The gap junctions are activated probabilistically. ξ_n denotes the probability of gap junction opening for the Ca^{2+} ions transition in the active interval. Assuming S_n gap junctions exist in between two touching cells, the number of open gap junctions s_n out of S_n gap junctions is modeled via the binomial distribution as

$$Pr\{s_n \text{ junctions open}\} = \binom{S_n}{s_n}\xi_n{}^{s_n}(1-\xi_n)^{S_n-s_n}. \quad (17)$$

For large S_n, the Binomial distribution can be approximated as Gaussian distribution:

$$s_n \sim \mathcal{N}(S_n\xi_n, S_n\xi_n(1-\xi_n)). \quad (18)$$

Considering both spatial and temporal dynamics, the Ca^{2+} wave injected to the nth cell after the gap junctional propagation is given by

$$\frac{\partial^2 C_{cyt}^{(n)}}{\partial x \partial t}|_{x=l_{jct}^{(n)}, t=\tau_{jct}^{(n)}} = \frac{s_n}{S_n}\theta_n C_{cyt}^{(n)}(l_{jct}^{-,n-1}, \tau_{jct}^{-,n-1}) \\ \delta(x - l_{jct}^{+,n}, t - \tau_{jct}^{+,n}) \quad (19)$$

where δ is the Dirac delta function. The received Ca^{2+} level after the gap junctional propagation is represented as

$$C_{cyt}^{(n)}(l_{jct}^{(n)}, \tau_{jct}^{(n)}) = \iint_{\mathcal{D}} \frac{\partial^2 C_{cyt}^{(n)}}{\partial x \partial t} dx dt \\ = \frac{s_n}{S_n}\theta_n C_{cyt}^{(n)}(l_{jct}^{-,n-1}, \tau_{jct}^{-,n-1}) \quad (20)$$

where $\mathcal{D} = [l_{jct}^{-,n}, l_{jct}^{+,n}] \times [\tau_{jct}^{-,n}, \tau_{jct}^{+,n}]$. The gain for the intercellular gap junctional propagation block is obtained as

$$\alpha_{inter}^{(n)} = \frac{E\{C_{cyt}^{(n)}(l_{jct}^{(n)}, \tau_{jct}^{(n)})\}}{C_{cyt}^{(n)}(l_{jct}^{-,n-1}, \tau_{jct}^{-,n-1})} \\ = \xi_n\frac{1}{\tau_{gap}^{(n)}}\frac{P_{Ca}^{(n)}}{D_{Ca}^{(n)}} \quad (21)$$

where E is the expectation operator.

C. Intracellular Diffusion Propagation

To model the spatial concentration propagation in the cell, the solution of the diffusion equation for a point source placed at the outlet of the gap junction is used. The diffusion equation relates the temporal concentration change in the concentration level to the spatial concentration change. The diffusion equation is given by

$$\frac{\partial C_{cyt}^{(n)}(x, t)}{\partial t} = D_{Ca}^{(n)}\frac{\partial^2 C_{cyt}^{(n)}(x, t)}{\partial x^2} \quad (22)$$

where $D_{Ca}^{(n)}$ is the Ca^{2+} diffusion constant for cytoplasm in the nth cell. $D_{Ca}^{(n)}$ captures the effects of cell boundaries and molecular crowding for intracellular diffusion propagation. The solution of the diffusion equation in (22) for a point source input is given by

$$C_{cyt}^{(n)}(x, t) = \frac{1}{\sqrt{4\pi D_{Ca}^{(n)}\tau_{cyt}^{(n)}}}e^{-(x^2/4D_{Ca}\tau_{cyt}^{(n)})} \quad (23)$$

where $\tau_{cyt}^{(n)}$ is the delay for propagation of Ca^{2+} in the cytoplasm.

To calculate the amount of Ca^{2+} traversing through the cell and reaching the neighboring cell, we use the solution of diffusion equation given in (23). We consider the delay $\tau_{intra}^{(n)}$ inside the cell required for the ions to reach to the gap junctions with the neighboring cell along the downstream propagation path.
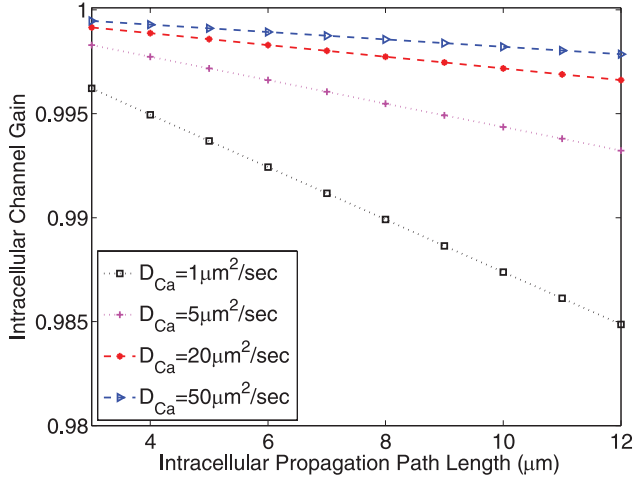
Fig. 4. Intracellular gain for the propagation through cytoplasm in (26) with respect to the different Ca^{2+} diffusion constant D_{Ca} values.

We also incorporate the gap junction opening duration $\tau_{\text{gap}}^{(n)}$. The delay of cytoplasmic propagation by diffusion is given by

$$\tau_{\text{cyt}}^{(n)} = \tau_{\text{intra}}^{(n)} + \tau_{\text{gap}}^{(n)} \tag{24}$$

where $\tau_{\text{intra}}^{(n)}$ can be obtained using the solution of the diffusion equation as [40]

$$\tau_{\text{intra}}^{(n)} = \frac{(l_{\text{cell}}^{(n)})^2}{2D_{\text{Ca}}^{(n)}} \tag{25}$$

where $l_{\text{cell}}^{(n)}$ is the intracellular propagation path length.

For the signal reception, we consider the propagation of the leading edge of the Ca^{2+} wave arriving at the gap junction region. Therefore, the channel gain $\alpha_{\text{intra}}^{(n)}$ for the intracellular propagation block is calculated for a delay of $\tau_{\text{intra}}^{(n)}$ as given in (24). Accordingly, we calculate the intracellular channel gain $\alpha_{\text{intra}}^{(n)}$ as the amount of Ca^{2+} concentration that reaches the gap junction region with the touching neighboring cell along the propagation path as

$$
\begin{aligned}
\alpha_{\text{intra}}^{(n)} \\
&= 2 \int_{l_{\text{cell}}^{(n)}}^{\infty} C_{\text{cyt}}^{(n)}(x, t)\mathrm{d}x \\
&= 2 \int_{l_{\text{cell}}^{(n)}}^{\infty} \frac{1}{\sqrt{4\pi D_{\text{Ca}}^{(n)}(\tau_{\text{intra}}^{(n)} + \tau_{\text{gap}}^{(n)})}} e^{-(x^2/4D_{\text{Ca}}(\tau_{\text{intra}}^{(n)}+\tau_{\text{gap}}^{(n)}))}\mathrm{d}x \\
&= 2Q\left(\frac{l_{\text{cell}}^{(n)}}{2D_{\text{Ca}}^{(n)}(\tau_{\text{intra}}^{(n)} + \tau_{\text{gap}}^{(n)})} \right) \tag{26}
\end{aligned}
$$

where Q($\cdot$) is the tail probability of the standard normal distribution.

In Fig. 4, the channel gain for the intracellular diffusion $\alpha_{\text{intra}}^{(n)}$ is studied based on (26). For different D_{Ca} values, the $\alpha_{\text{intra}}^{(n)}$ is equal to ≈ 1, when the intracellular propagation path length l_{cell} is varied from 3 to 12 μm. Therefore, for the considered cell length and Ca^{2+} diffusion constant ranges, the effect of intracellular diffusion propagation is found to be not consequential.

D. Noise Analysis

The cytoplasmic Ca^{2+} elevation is composed of contribution of calcium intake from various elements in the intracellular Ca^{2+} signaling pathway. For example, in the model we adopted for Ca^{2+} wave generation [33], the cytoplasmic Ca^{2+} is contributed by the Ca^{2+} of the extracellular space, the buffer proteins, the Ca^{2+} store (organelles). Therefore, the total cytoplasmic Ca^{2+} can be expressed via addition of contributions from the different elements as

$$\lim_{t \to \infty} C_{\text{cyt}}(t) = \sum_{g=1}^{G} \lim_{t \to \infty} C_{\text{cyt}}^{(g)}(t) \tag{27}$$

where $C_{\text{cyt}}^{(g)}(t)$ represents the contribution from the different element g, and G is the total number of elements in the intracellular Ca^{2+} signaling pathway for the Ca^{2+} wave generation.

The chemical reactions can be modeled using Poisson distribution [41]. Therefore, each contributor to the Ca^{2+} elevation can be taken as Poisson distributed random variable.

$$C_{\text{cyt}}^{(g)}(t) \sim \text{Pois}\{\lambda_g\}. \tag{28}$$

The total Ca^{2+} concentration becomes the outcome of addition from multiple Poisson sources. These processes are assumed to be independent. The addition of the independent Ca^{2+} random sources can be approximated as Gaussian distributed by law of large numbers as

$$\lim_{G \to \infty} \frac{1}{\sqrt{G}} \sum_{g=1}^{G} \frac{C_{\text{cyt}}^{(g)}(t) - \lambda_g}{\sqrt{\lambda_g}} \sim \mathcal{N}\{0, 1\}. \tag{29}$$

The generation noise can be taken as Gaussian distributed as

$$
\begin{aligned}
\lim_{t \to \infty} C_{\text{cyt}}(t) &\sim \mathcal{N}\{\eta, \sigma_{\text{gen}}^2\} \\
&= \eta + w_{\text{gen}} \tag{30}
\end{aligned}
$$

where w_{gen} represents the generation noise, given by

$$w_{\text{gen}} \sim \mathcal{N}\{0, \sigma_{\text{gen}}^2\}. \tag{31}$$

Additionally, to incorporate the noise effects at the receiver side, where the measurements of Ca^{2+} signal are taken, an additive noise factor w_{recv} is incorporated into the model, which is defined as

$$w_{\text{recv}} \sim \mathcal{N}\{0, \sigma_{\text{recv}}^2\}. \tag{32}$$

Next, the overall noisy linear channel model is presented.

E. End-to-End Model

Here, we utilize the developed blocks of Ca^{2+} generation, gap junctional propagation, and intracellular propagation to provide a linear relation between the generated Ca^{2+} wave level η and the received signal ψ. To this end, the end-to-end channel gain is calculated based on the shortest delay path between the cell Ca^{2+} wave generated and the last cell where the samples are taken. N is the number of cells in the shortest delay path between the transmitter and the receiver. The received signal ψ is given by

$$\psi = \prod_{n=1}^{N} \alpha_{\text{intra}}^{(n)} \alpha_{\text{inter}}^{(n)}(\eta + w_{\text{gen}}) + w_{\text{recv}} \tag{33}$$

where η is given as a function of the extracellular Ca^{2+} concentration in (8), $\alpha_{\text{inter}}^{(n)}$ is as given in (21), and $\alpha_{\text{intra}}^{(n)}$ is given as in (26). The addition of the intracellular propagation delay and the gap junctional delay is large enough that Ca^{2+} wave generation block reaches the steady state before propagating through the gap junctions to the next cell on the shortest delay path. The end-to-end delay is given by

$$\tau_{\text{total}} = \tau_{\text{gen}} + \sum_{n=2}^{N} \tau_{\text{intra}}^{(n)} + \tau_{\text{gap}}^{(n)}. \tag{34}$$

Next, we analyze the bit error probability for intra/inter-cellular Ca^{2+} MC utilizing the developed linear end-to-end channel model.

IV. BIT ERROR PROBABILITY ANALYSIS FOR MC WITH INTERCELLULAR Ca^{2+} WAVES

In this section, we study the bit error probability in MC with Ca^{2+} waves. First, the error probability is given for binary pulse-amplitude modulation (PAM) transmission. Then, the impact of the distance between the pulse levels on the bit error rate is investigated.

A. Binary Transmission

We study the probability of error for the PAM input signals. For the transmission of different information, each different input pulse level is labeled as η_i, where index i indicates which information, i.e., symbol, was transmitted.

The received signal ψ is obtained via sampling the Ca^{2+} at the receiver side. The distribution of the received signal ψ for the transmitted information symbol i is represented as

$$p(\psi|\eta_i) \sim \mathcal{N}(\mu_i, \sigma_i^2) \tag{35}$$

where μ_i is obtained using (33) as

$$\mu_i = \prod_{n=1}^{N} \xi_n \theta_n \eta_i \tag{36}$$

and σ_i^2 is

$$\sigma_i^2 = \prod_{n=1}^{N} \xi_n^2 \theta_n^2 \sigma_{\text{gen}}^2 + \sigma_{\text{recv}}^2. \tag{37}$$

In the following, we formulate the probability of error for the binary PAM Ca^{2+} signals.

For the binary transmission case, only two different Ca^{2+} signal levels, i.e., η_1 and η_2, are considered to be transmitted. During the formulation, the corresponding signal level to η_1 is taken to be lower than the one for η_2. In the line with signal levels, the Ca^{2+} signal received for η_1 is lower than η_2. The probability distribution of the received signal for η_1 is as

$$p(\psi|\eta_1) = \frac{1}{\sqrt{2\pi\sigma_1^2}} e^{-((\psi-\mu_1)^2/2\sigma_1^2)} \tag{38}$$

and for the transmission signal level corresponding to η_2, the distribution of the received signal is given as

$$p(\psi|\eta_2) = \frac{1}{\sqrt{2\pi\sigma_2^2}} e^{-((\psi-\mu_2)^2/2\sigma_2^2)}. \tag{39}$$

The probability of error for η_1, i.e., the received signal greater than the detection threshold ζ, is given by

$$P(\psi > \zeta|\xi^N\theta^N\eta_1) = \int_{\zeta}^{\infty} p(\psi|\xi^N\theta^N\eta_1)\mathrm{d}\psi \tag{40}$$

and similarly the probability of error for η_2 is given by

$$P(\psi < \zeta|\xi^N\theta^N\eta_2) = \int_{-\infty}^{\zeta} p(\psi|\xi^N\theta^N\eta_2)\mathrm{d}\psi. \tag{41}$$

Under equally likely transmission probability for both signals, the probability of error for binary PAM is obtained using (40) and (41) by

$$P_b = P(\psi > \zeta|\xi^N\theta^N\eta_1) + P(\psi < \zeta|\xi^N\theta^N\eta_2). \tag{42}$$

B. Selection of the Detection Threshold

Here, we formulate the probability of error as a function of the difference between the detection threshold ζ and the mean received signal $E\{\psi\}$ to further investigate the impact of the detection threshold on error performance via numerical results. We assume that cells have identical biophysical parameters, i.e., $\theta_1 = \theta_2 = \cdots = \theta_N$ and $\xi_1 = \xi_2 = \cdots = \xi_N$. The different between the detection threshold ζ and received signal for the transmission level η_1 is equal to $\zeta - \xi^N\theta^N\eta_1$. Based on the probability of error given in (40), we refine the probability of error for the transmission of η_1 as

$$\begin{aligned} P(\psi > \zeta|\xi^N\theta^N\eta_1) &= P(\psi > \zeta|\xi^N\theta^N\eta_1) \\ &= P(\psi > \zeta - \xi^N\theta^N\eta_1|\xi^N\theta^N\eta_1 \\ &\quad - \xi^N\theta^N\eta_1) \\ &= P(\psi > \zeta - \xi^N\theta^N\eta_1|0). \end{aligned} \tag{43}$$

Accordingly, the probability of error for η_1, i.e., $P(\psi > \zeta_1|\eta_1)$ is given as a function of $\zeta - \xi^N\theta^N\eta_1$ by

$$\begin{aligned} P(\psi > \zeta - \xi^N\theta^N\eta_1|0) &= \int_{\zeta-\xi^N\theta^N\eta_1}^{\infty} p(\psi|0)\mathrm{d}\psi \\ &= \int_{\zeta-\xi^N\theta^N\eta_1}^{\infty} \frac{1}{\sqrt{2\pi\sigma_1^2}} e^{-(\psi^2/2\sigma_1^2)}\mathrm{d}\psi \\ &= Q\left(\frac{\zeta - \xi^N\theta^N\eta_1}{\sigma_1^2}\right) \end{aligned} \tag{44}$$

where $Q(\cdot)$ is the tail probability distribution of the standard normal distribution. Next, we provide numerical results to elaborate the channel characteristics and error performance for end-to-end intra/inter-cellular Ca^{2+} MC.

V. NUMERICAL RESULTS

In this section, we study the MC with intercellular Ca^{2+} waves via numerical results. The analytical expressions obtained in Sections III and IV are evaluated here. The values of biophysical system parameters are used as given in Table I if not otherwise noted. For illustration purposes of numerical results, we assume all cells ($n = 1, \ldots, N$) have the same values for the biophysical parameters. The values of the biophysical parameters are selected based on the values in [33], [42]–[44].
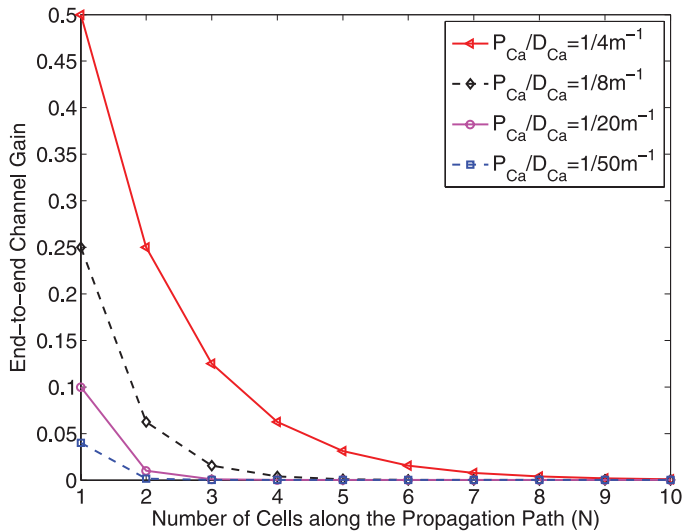
Fig. 5. The end-to-end channel gain with respect to distance for different P_{Ca}/D_{Ca} ratios of 1/4, 1/8, 1/20, and 1/50 m^{-1}.

Fig. 6. The impact of the gap junctional delay τ_{gap} on the end-to-end channel gain. The end-to-end channel gain is tested for $\tau_{gap} = 0.15, 0.2, 0.4$ and 0.6 s.

A. End-to-End Model

1) End-to-End Channel Gain: Here, we study the end-to-end channel gain $\prod_{n=1}^{N} \alpha_{intra}^{(n)} \alpha_{inter}^{(n)}$, which is based on the received signal model presented in (33). In Fig. 5, the impact of the cytoplasmic diffusion constant (D_{Ca}) and the gap junctional permeability (P_{Ca}) of Ca^{2+} for the end-to-end channel gain is studied. ξ is set to 4/5, and τ_{gap} is set to 400 ms. The P_{Ca} is taken as 5×10^{-6} m/s for the D_{Ca} of 20×10^{-6} m^2/s, 40×10^{-6} m^2/s, 100×10^{-6} m^2/s, and 250×10^{-6} m^2/s. The intercellular channel gain is shown to be proportional to the ratio of P_{Ca}/D_{Ca} in (21). Using the formulation in (33), the end-to-end channel gain is investigated with respect to the P_{Ca}/D_{Ca} ratio. It is observed that as the D_{Ca} increases, the end-to-end channel gain decreases, i.e., the attenuation increases. The decreasing P_{Ca}/D_{Ca} ratio also enables information transmission over higher number of cells along the propagation path.

In Fig. 6, the impact of the gap junctional delay τ_{gap} on the end-to-end channel gain is investigated for MC with intercellular Ca^{2+} waves. P_{Ca} is taken as 5×10^{-6} m/s, D_{Ca} is taken as 50×10^{-6} m^2/s, ξ is set to 4/5. τ_{gap} is tested for values of 0.15, 0.2, 0.4, and 0.6 s. As the gap junctional delay τ_{gap} increases, the intercellular propagation gain increases as well in (21). Using the formulation in (33), the end-to-end channel gain is investigated with respect to the τ_{gap}. It is observed that the higher the gap junctional delay, the higher the end-to-end channel gain. As the gap junctions are open for a longer time interval, the number of cells the Ca^{2+} wave can travel increases for a given requirement on the level of the received signal.

In Fig. 7, the impact of the successful gap junction opening probability ξ on the end-to-end channel gain is illustrated. P_{Ca} is taken as 5×10^{-6} m/s, D_{Ca} is taken as 20×10^{-6} m^2/s, and τ_{gap} is set to 400 ms. ξ is tested for values of 1/5, 1/2, 3/5, and 9/10. The intercellular propagation gain proportionally increases with the gap junction successful opening probability
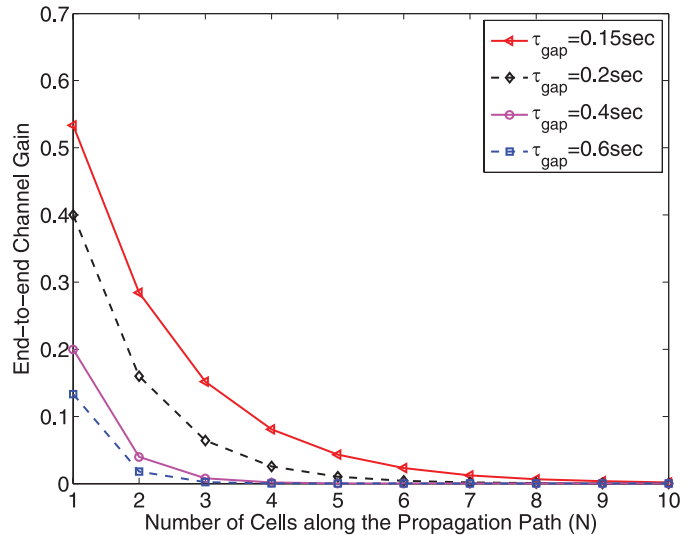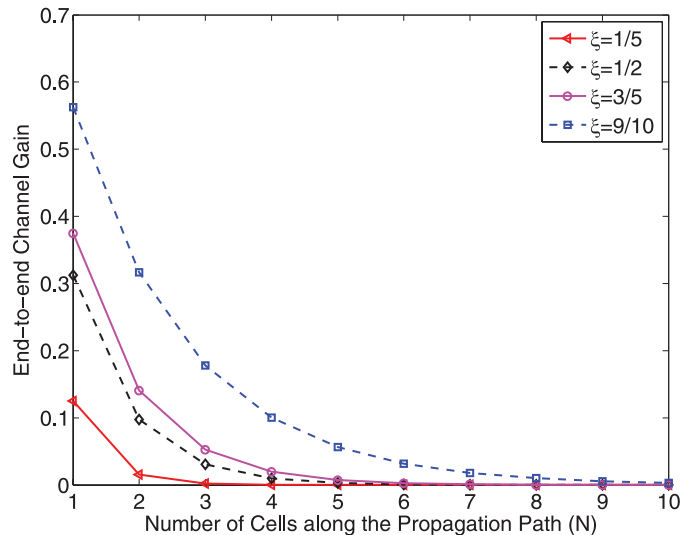

Fig. 7. The impact of the probability of gap junction opening ξ on the end-to-end channel gain with respect to the distance. The end-to-end channel gain is tested for $\xi = 1/5, 1/2, 3/5$ and $9/10$.

ξ in (21). Using the formulation in (33), the end-to-end channel gain is investigated with respect to the ξ. It is observed that as the ξ increases, the end-to-end channel gain improves. The enhanced end-to-end channel gain with the increasing ξ provides ability to communicate over larger number of cells along the propagation path.

In addition, the sharp decay of the end-to-end gain after several cells in Figs. 5–7 can be attributed to the developed non-regenerative model of Ca^{2+} wave propagation in this work.

2) End-to-End Delay: In Fig. 8, the results on the end-to-end delay for different C_{ext} values of 1500, 2500, and 3500 μM are presented. l_{cell} is 5 μm, D_{Ca} is 50×10^{-6} m^2/s, τ_{gap} is set to 400 ms, and β is taken 10 s^{-1}. The end-to-end delay is given in (34). It is observed that higher C_{ext} yields
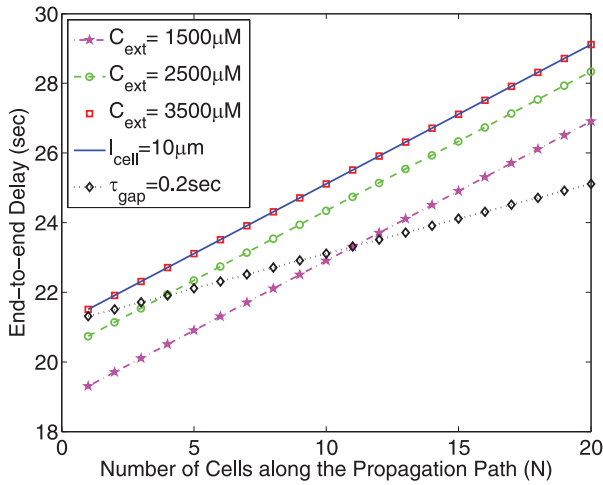
Fig. 8. The end-to-end delay τ_{total} with respect to the number of cells along the propagation path (N). C_{ext} is tested for 3 different values of 1500, 2500, and 3500 μM. Furthermore, the impact of the cell length l_{cell} and gap junctional delay τ_{gap} are illustrated in blue and black colored lines for $C_{\text{ext}} = 3500$ μM.
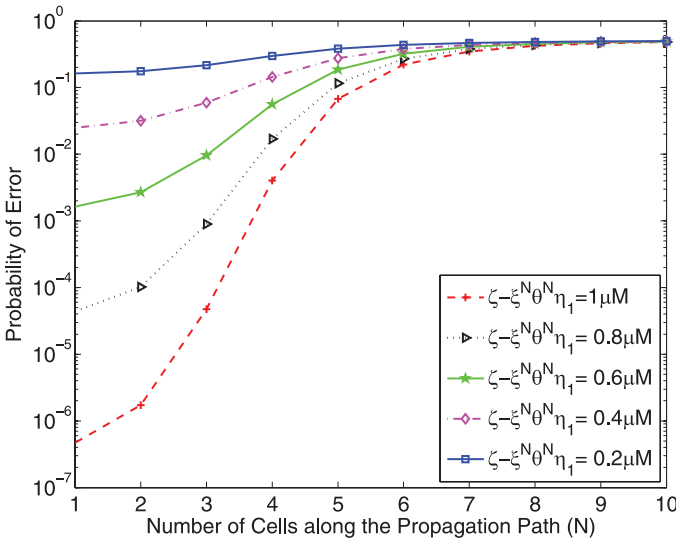

Fig. 9. The impact of the level difference between the pulse levels on the bit error probability for binary information transmission with intercellular Ca^{2+} waves.

higher end-to-end delay. These results can be attributed to the higher Ca^{2+} delay for higher C_{ext} values. For all C_{ext} values the end-to-end delay follows similar pattern. Furthermore, for $C_{\text{ext}} = 3500$ μM, the intracellular propagation path length l_{cell} is increased to 10 μm. The impact of the l_{cell} increase on the end-to-end delay τ_{total} is shown to be negligible, since the curves for 5 μm and 10 μm are overlapping. Additionally, the impact of gap junctional delay τ_{gap} is assessed by reducing it to 0.2 s. The exposed end-to-end delay reduces with the reduced τ_{gap} from 0.4 s to 0.2 s.

B. Bit Error Probability

In Fig. 9, the impact of the difference between the detection threshold ζ and the mean of the received signal $E\{\psi\}$ on the bit error probability is illustrated. The mean of the received signal for the transmission of the information η_1 is given by $\xi^N \theta^N \eta_1$. ξ is set to 4/5, P_{Ca} is taken as 5 μm/s, D_{Ca} is taken as 20 μm^2/s, τ_{gap} is taken as 400 ms, σ_{gen}^2 is 10^{-14} μM^2, and σ_{recv}^2 is 10^{-16} μM^2. Using the formulation in (44), the bit error probability is investigated for various values of the difference $\zeta - \xi^N \theta^N \eta_1$. It is observed that the probability of error is significantly amplified as the number of cells along the propagation path increases by a few more cells. To have a bit error probability less than 10^{-3}, the difference $\zeta - \xi^N \theta^N \eta_1$ needs to be about 0.8 μM or larger even for $N = 4$.

VI. CONCLUSION

In this paper, the intra/inter-cellular Ca^{2+} signaling mechanisms are studied for information transmission over consecutive cells touching each other. First, a linear channel model is developed for the intra/inter-cellular Ca^{2+} MC. A theoretical framework incorporating the biophysical dynamics of the Ca^{2+} wave generation, gap junctional propagation, and intracellular propagation is provided. To the best of our knowledge, this is the first work on the development of a linear channel model for the intra/inter-cellular Ca^{2+} MC. Then, the bit error probability for binary transmission is investigated. Numerical results point out the limited propagation distance for MC with intercellular Ca^{2+} waves, which is limited to several tens of cells. The modeling framework and the results obtained in this study are aimed to facilitate the development of MC systems using the intracellular and intercellular Ca^{2+} signals for information transfer. Furthermore, the reverse engineering of biological Ca^{2+} signaling systems can also benefit the understanding of causes for many prominent diseases due to the Ca^{2+} signaling dependent homeostatic variations. Future work includes validation of the developed model and extension to address three-dimensional cell networks.

REFERENCES

[1] I. F. Akyidliz, J. M. Jornet, and M. Pierobon, "Nanonetworks: A new frontier in communications, " *Commun. ACM*, vol. 54, no. 11, pp. 84–89, Nov. 2011.

[2] B. D. Unluturk, A. O. Bicen, and I. F. Akyildiz, "Genetically engineered bacteria-based transceivers for molecular communication, " *IEEE Trans. Commun.*, vol. 63, no. 4, pp. 1271–1281, Apr. 2015.

[3] A. O. Bicen, C. M. Austin, I. F. Akyildiz, and C. R. Forest, "Efficient sampling of bacterial signal transduction for detection of pulse-amplitude modulated molecular signals, " *IEEE Trans. Biomed. Circuits Syst.*, vol. 9, no. 4, pp. 505–517, Aug. 2015.

[4] M. Moore, A. Enomoto, T. Nakano, R. Egashira, T. Suda, A. Kayasuga, H. Kojima, H. Sakakibara, and K. Oiwa, "A design of a molecular communication system for nanomachines using molecular motors, " in *Proc. IEEE Int. Conf. Pervasive Comput. Commun. Workshops (PERCOMW)*, 2006.

[5] Y. Chahibi and I. Balasingham, "Channel modeling and analysis for molecular motors in nano-scale communications, " in *Proc. ACM NANOCOM*, Boston, MA, USA, Sep. 2015.

[6] D. Kilinc and O. B. Akan, "An information theoretical analysis of nanoscale molecular gap junction communication channel between cardiomyocytes, " *IEEE Trans. Nanotechnol.*, vol. 12, no. 2, pp. 129–136, Mar. 2013.

[7] L. Gine and I. F. Akyildiz, "Molecular communication options for long range nanonetworks, " *Comput. Netw. (Elsevier)*, vol. 53, no. 16, pp. 2753–2766, Nov. 2009.

[8] T. M. Allen and P. R. Cullis, "Drug delivery systems: Entering the mainstream, " *Nature*, vol. 303, no. 5665, pp. 1818–1822, Mar. 2004.

[9] Y. Chahibi and I. F. Akyildiz, "A molecular communication system model for particulate drug delivery systems, " *IEEE Trans. Biomed. Eng.*, vol. 60, no. 12, pp. 3468–3483, Dec. 2013.

[10] M. Pierobon and I. F. Akyildiz, "Noise analysis in ligand-binding reception for molecular communication in nanonetworks, " *IEEE Trans. Signal Process.*, vol. 59, no. 9, pp. 4168–4182, Sep. 2011.

[11] T. Nakano, T. Suda, M. Moore, R. Egashira, A. Enomoto, and K. Arima, "Molecular communication for nanomachines using intercellular calcium signaling, " in *Proc. IEEE Conf. Nanotechnol.*, Nagoya, Japan, Jul. 2005.

[12] A. Goldbeter, *Biochemical Oscillations and Cellular Rhythms*. Cambridge, U.K.: Cambridge Univ. Press, 1996.

[13] M. J. Berridge, M. D. Bootman, and P. Lipp, "Calcium–A life and death signal, " *Nature*, vol. 395, no. 6703, pp. 645–648, Oct. 1998.

[14] M. Berridge, P. Lipp, and M. Bootman, "Calcium signalling, " *Curr. Biol.*, vol. 9, no. 5, pp. R157–R159, Mar. 1999.

[15] K. T. Jones, "Ca^{2+} oscillations in the activation of the egg and development of the embryo in mammals, " *Int. J. Dev. Biol.*, vol. 42, no. 1, pp. 1–10, Jan. 1998.

[16] B. Soria and F. Martin, "Cytosolic calcium oscillations and insulin release in pancreatic islets of Langerhans, " *Diabet. Metab.*, vol. 24, no. 1, pp. 37–40, Feb. 1998.

[17] I. Schulz, E. Krause, A. A. Gonzalez, A. Gobel, L. Sternfeld, and A. Schmid, "Agonist-stimulated pathways of calcium signaling in pancreatic acinar cells, " *Biol. Chem.*, vol. 380, no. 7–8, pp. 903–908, Jul.-Aug. 1999.

[18] M. R. McAinsh, A. A. R. Webb, J. E. Taylor, and A. M. Hetherington, "Stimulus-induced oscillations in guard cell cytosolic free calcium, " *Plant Cell*, vol. 7, no. 8, pp. 1207–1219, Aug. 1995.

[19] M. Koenigsberger, D. Seppey, J.-L. Beny, and J.-J. Meister, "Mechanisms of propagation of intercellular calcium waves in arterial smooth muscle cells, " *Biophys. J.*, vol. 99, no. 2, pp. 333–343, Jul. 2010.

[20] K. Morita, K. Koketsu, and K. Kuba, "Oscillation of $[Ca^{2+}]_i$ -linked K^+ conductance in bullfrog sympathetic ganglion cell is sensitive to intracellular anions, " *Nature*, vol. 283, no. 5743, pp. 204–205, Jan. 1980.

[21] K. S. R. Cuthbertson and P. H. Cobbold, "Phorbol ester and sperm activate mouse oocytes by inducing sustained oscillations in cell Ca^{2+}, " *Nature*, vol. 316, pp. 541–542, 1985.

[22] N. M. Woods, K. S. R. Cuthbertson, and P. H. Cobbold, "Repetitive transient rises in cytoplasmic free calcium in hormone-stimulated hepatocytes, " *Nature*, vol. 319, no. 6054, pp. 600–602, Feb. 1986.

[23] N. M. Woods, K. S. R. Cuthbertson, and P. H. Cobbold, "Agonist-induced oscillations in cytoplasmic free calcium concentration in single rat hepatocytes, " *Cell Calcium*, vol. 8, no. 1, pp. 79–100, Feb. 1987.

[24] J. T. Russel, "Imaging calcium signals in vivo: A powerful tool in physiology and pharmacology, " *Brit. J. Pharmacol.*, vol. 163, no. 8, pp. 1605–1625, Aug. 2011.

[25] I. F. Akyildiz, M. Pierobon, S. Balasubramaniam, and Y. Koucheryavy, "Internet of bio-nano things, " *IEEE Commun. Mag.*, vol. 53, no. 3, pp. 32–40, Mar. 2015.

[26] M. J. Berridge, M. D. Bootman, and H. L. Roderick, "Calcium signaling: Dynamics, homeostasis and remodelling, " *Nat. Rev. Mol. Cell Biol.*, vol. 4, no. 7, pp. 517–529, Jul. 2003.

[27] S. Schuster, M. Marhl, and T. Hofer, "Modeling of simple and complex calcium oscillations, " *Eur. J. Biochem.*, vol. 269, no. 5, pp. 1333–1355, Mar. 2002.

[28] M. S. Kuran, T. Tugcu, and B. Ozerman, "Calcium signaling: Overview and research directions of a molecular communication paradigm, " *IEEE Wireless Commun. Mag.*, vol. 19, no. 5, pp. 20–27, Oct. 2012.

[29] T. Nakano and J.-Q. Liu, "Design and analysis of molecular relay channels: An information theoretic approach, " *IEEE Trans. NanoBiosci.*, vol. 9, no. 3, pp. 213–221, Sep. 2010.

[30] M. T. Barros, S. Balasubramaniam, and B. Jennings, "Comparative end-to-end analysis of Ca^{2+} signaling-based molecular communication in biological tissues," *IEEE Trans. Commun.*, vol. 63, no. 12, pp. 5128–5142, Dec. 2015.

[31] H. L. Van Trees, *Detection, Estimation, and Modulation Theory, Part I*. New York: Wiley, 1968.

[32] T. M. Cover and J. A. Thomas, *Elements of Information Theory*. New York: Wiley-Interscience, 2006.

[33] A. Korngreen, V. Gold'shtein, and Z. Priel, "A realistic model of biphasic calcium transients in electrically nonexcitable cells, " *Biophys. J.*, vol. 73, no. 2, pp. 659–673, Aug. 1997.

[34] T. Hofer, "Model of intercellular calcium oscillations in hepatocytes: Synchronization of heterogeneous cells, " *Biophys. J.*, vol. 77, no. 3, pp. 1244–1256, Sep. 1999.

[35] L. Venance, N. Stella, J. Glowinski, and C. Giaume, "Mechanism involved in initiation and propagation of receptor-induced intercellular calcium signaling in cultured rat astrocytes, " *J. Neurosci.*, vol. 17, no. 6, pp. 1981–1992, Mar. 1997.

[36] T. Hofer, L. Venance, and C. Giaume, "Control and plasticity of intercellular calcium waves in astrocytes: A modeling approach, " *J. Neurosci.*, vol. 22, no. 12, pp. 4850–4859, Jun. 2002.

[37] C. Schofl, G. Brabant, R. D. Hesch, A. von zur Muhlen, P. H. Cobbold, and K. S. R. Cuthbertson, "Temporal patterns of alpha 1-receptor stimulation regulate amplitude and frequency of calcium transients, " *Amer. J. Physiol.*, vol. 265, pp. C1030–C1036, 1993.

[38] R. E. Dolmetsch, R. S. Lewis, C. C. Goodnow, and J. I. Healy, "Differential activation of transcription factors induced by Ca^{2+} response amplitude and duration, " *Nature*, vol. 386, no. 6627, pp. 855–858, Apr. 1997.

[39] K. Prank, F. Gabbiani, and G. Brabant, "Coding efficiency and information rates in transmembrane signaling, " *Biosystems*, vol. 55, no. 1–3, pp. 15–22, Feb. 2000.

[40] A. O. Bicen and I. F. Akyildiz, "End-to-end propagation noise and memory analysis for molecular communication over microfluidic channels, " *IEEE Trans. Commun.*, vol. 62, no. 7, pp. 2432–2443, Jul. 2014.

[41] D. T. Gillespie, "Stochastic simulation of chemical kinetics, " *Annu. Rev. Phys. Chem.*, vol. 58, pp. 35–55, May 2007.

[42] N. L. Allbritton, T. Meyer, and L. Stryer, "Range of messenger action of calcium ion and inositol 1, 4, 5-trisphosphate, " *Science*, vol. 258, no. 5089, pp. 1812–1815, Dec. 1992.

[43] V. Verselis, R. L. White, D. C. Spray, and M. V. Bennett, "Gap junctional conductance and permeability are linearly related, " *Science*, vol. 234, no. 4775, pp. 461–464, Oct. 1986.

[44] R. Eckert, B. Adams, J. Kistler, and P. Donaldson, "Quantitative determination of gap junctional permeability in the lens cortex, " *J. Membr. Biol.*, vol. 169, no. 2, pp. 91–102, May 1999.

A. Ozan Bicen (S'08) received the B.Sc. and M.Sc. degrees in electrical and electronics engineering from Middle East Technical University, Ankara, Turkey, in 2010 and from Koc University, Istanbul, Turkey, in 2012, respectively. He received the Ph.D. degree in electrical and computer engineering from Georgia Institute of Technology, Atlanta, GA, USA, in May 2016. His current research interests include molecular communication, biomedical signal processing, and wireless communications.

Ian F. Akyildiz (M'86–SM'89–F'96) received the B.S., M.S., and Ph.D. degrees in computer engineering from the University of Erlangen-Nurnberg, Germany, in 1978, 1981, and 1984, respectively. Currently, he is the Ken Byers Chair Professor in Telecommunications with the School of Electrical and Computer Engineering, Georgia Institute of Technology, Atlanta, GA, USA, the Director of the Broadband Wireless Networking Laboratory and Chair of the Telecommunication Group at Georgia Tech. Since September 2012, Dr. Akyildiz is also a FiDiPro Professor (Finland Distinguished Professor Program (FiDiPro) supported by the Academy of Finland) at Tampere University of Technology, Department of Communications Engineering, Finland. He received numerous awards from IEEE and ACM. His current research interests are in nanonetworks, Long Term Evolution (LTE) advanced networks, cognitive radio networks, and wireless sensor networks.

Sasitharan Balasubramaniam (SM'14) received the B.S. degree in electrical and electronic engineering and the Ph.D. degree from the University of Queensland, Australia, in 1999 and 2005, respectively, and the M.S. degree in computer and communication engineering from the Queensland University of Technology, Australia, in 1999. Currently, he is an Academy of Finland Research Fellow with the Nano Communication Centre, Department of Electronic and Communication Engineering, Tampere University of Technology, Tampere, Finland. His research interests include bio-inspired communication networks, and molecular communications. Currently, he is an Editor for the IEEE INTERNET OF THINGS JOURNAL, *Nano Communication Networks*, *Swarm and Evolutionary Computation*, and *Digital Communication and Networks*.

Yevgeni Koucheryavy received the Ph.D. degree from the Tampere University of Technology (TUT), Finland in 2004. He is a Professor and Lab Director at the Department of Electronics and Communications Engineering at the TUT. He is the author of numerous publications in the field of advanced wired and wireless networking and communications. His current research interests include various aspects in heterogeneous wireless communication networks and systems, the Internet of Things, and nanocommunications. He is an Associate Technical Editor of IEEE *Communications Magazine* and Editor of IEEE *Communications Surveys and Tutorials*.